Smart Structures and Systems, *Vol. 18, No. 3 (2016) 449-470*
DOI: http://dx.doi.org/10.12989/sss.2016.18.3.449

Electromagnetic energy harvesting from structural vibrations during earthquakes

Wenai Shen[1a], Songye Zhu[*2], Hongping Zhu[1b] and You-lin Xu[2c]

[1]*School of Civil Engineering and Mechanics, Huazhong University of Science and Technology, Wuhan 430074, China*
[2]*Department of Civil and Environmental Engineering, The Hong Kong Polytechnic University, Kowloon, Hong Kong*

(Received May 30, 2015, Revised August 8, 2015, Accepted August 20, 2015)

Abstract. Energy harvesting is an emerging technique that extracts energy from surrounding environments to power low-power devices. For example, it can potentially provide sustainable energy for wireless sensing networks (WSNs) or structural control systems in civil engineering applications. This paper presents a comprehensive study on harvesting energy from earthquake-induced structural vibrations, which is typically of low frequency, to power WSNs. A macroscale pendulum-type electromagnetic harvester (MPEH) is proposed, analyzed and experimentally validated. The presented predictive model describes output power dependence with mass, efficiency and the power spectral density of base acceleration, providing a simple tool to estimate harvested energy. A series of shaking table tests in which a single-storey steel frame model equipped with a MPEH has been carried out under earthquake excitations. Three types of energy harvesting circuits, namely, a resistor circuit, a standard energy harvesting circuit (SEHC) and a voltage-mode controlled buck-boost converter were used for comparative study. In ideal cases, i.e., resistor circuit cases, the maximum electric energy of 8.72 J was harvested with the efficiency of 35.3%. In practical cases, the maximum electric energy of 4.67 J was extracted via the buck-boost converter under the same conditions. The predictive model on output power and harvested energy has been validated by the test data.

Keywords: vibration energy harvesting; earthquake; circuit; predictive model; low frequency; shaking table test

1. Introduction

Wireless sensing is increasingly deployed in bridges and tall buildings for structural health monitoring (SHM) due to its low cost, easy deployment and on-line signal processing functionality (Lynch and Loh 2006, Spencer *et al.* 2011, Lei *et al.* 2012, Shen *et al.* 2012). However, power supplies to wireless sensor networks (WSNs) remains a critical concern after removing traditional power cables. Batteries are often used as local power supplies to WSNs. However, the limited

∗Corresponding author, Associate Professor, E-mail: songye.zhu@polyu.edu.hk
[a] Assistant Professor, E-mail: wshen@hust.edu.cn
[b] Professor, E-mail: hpzhu@mail.hust.edu.cn
[c] Chair Professor, E-mail: you-lin.xu@polyu.edu.hk

http://www.techno-press.org/?journal=sss&subpage=8 ISSN: 1738-1584 (Print), 1738-1991 (Online)

lifetime of batteries unavoidably requires frequent replacements, resulting in high maintenance cost and low efficiency. In view of this, powering WSNs using energy harvesting technique has been proposed to fulfill the concept of ‘energy autonomy’ or ‘autonomous WSNs’ (Roundy *et al.* 2003, Mahlknecht 2004, Park *et al.* 2008, Vullers *et al.* 2010, Harb 2011, Alavi *et al.* 2016). Autonomous energy-scavenging sensor technique is highlighted as one of the six emerging technologies in the coming decade by *Nature* (Van Noorden 2012).

Energy harvesting for autonomous WSNs aims to exploit efficient, reliable, and robust localized power generation (Shen 2014). Solar, wind, radio-frequency waves, and ambient vibrations are available power sources for WSNs applied in civil structures. Solar energy harvesting using photovoltaic panels and wind energy harvesting using small wind turbines can provide sufficient power to WSNs, although their operations greatly depend on weather conditions. Spencer *et al.* (2011) successfully performed wind and solar energy harvesting to power the wireless smart monitoring system in the Jindo Bridge in Korea.

Vibration energy harvesting seems to be another rational choice, especially for wireless sensors installed on structures subjected to regular vibrations under traffic or wind excitations. Piezoelectric and electromagnetic harvesters are two major types of vibration energy harvesters. Piezoelectric harvesters are often preferred in microscale applications because of their convenient fabrications. Elvin *et al.* (2006) investigated a small-scale (5 cm^3) piezoelectric harvester with a cantilever-beam configuration and a proof mass of 25 g as a potential power source for wireless sensors. Experimental results show that the 5 cm^3 piezoelectric harvester connected to a resistor circuit can generate 0.49 μJ energy under 50s El Centro earthquake excitation. The typical working frequency of lead zirconate titanate (PZT) bimorph energy harvesters is up to hundreds of Hz or above, which exceeds the frequency range of structural responses (Rhimi and Lajnef 2012). However, piezoelectric polymers, e.g., semi-crystalline plastic polyvinylidene fluoride (PVDF), can work more effectively at a low frequency due to their flexibilities, and thus are attracting increasing attention for energy harvesting applications (Lajnef *et al.* 2008, Ramadan *et al.* 2014).

Electromagnetic energy harvesting is a promising technique suitable for the applications in civil structures in view that structural dynamic responses typically ranges from 0.1 Hz to 20 Hz. Casciati and Rossi (2007) proposed an electromagnetic harvester with high-impedance feature to convert the mechanical energy of structures into electricity. Sazonov *et al.* (2009) conducted field test of an electromagnetic harvester that scavenges the vibration energy induced by passing vehicles. Electromagnetic harvesters were also proposed to scavenge the wind-induced vibration energy of bridge stay cables (Jung *et al.* 2011, Jung *et al.* 2012, Kim *et al.* 2013, Shen and Zhu 2015). Jung *et al.* (2012) proposed an electromagnetic harvester to scavenge vibration energy of bridge stay cables, and the performance of the harvester was validated via shaking table tests and field tests. In addition, simultaneous vibration damping and energy harvesting using electromagnetic devices were proposed recently by the writers of this paper (Zhu *et al.* 2012, Shen *et al.* 2012, Shen and Zhu 2015). Based on this concept, a self-powered vibration control and monitoring system was developed, in which a wireless sensor was successfully powered by the energy output from an electromagnetic tuned mass damper (Shen *et al.* 2012). Shen and Zhu (2015) conducted a numerical study on the dual-function electromagnetic device in an application to an actual stay cable in Hong Kong Stonecutters Bridge. Numerical results show that the electromagnetic device produces average output power of several watts when the stay cable is subjected to buffeting-induced vibration.

Meanwhile, harvesting vibration energy of civil structures subjected to earthquake ground motions attracts increasingly attention from the community. The main purpose is to provide electrical energy to sensing systems or structural control systems when regular power supplies are unavailable in such extreme events (Sapiński 2011, Lu *et al.* 2014). Scruggs (1999) proposed a regenerative active mass damper, which used a permanent-magnet machine to harvest vibration energy to power an actuator for seismic protection of structures. Auge (2003) proposed a concept of energy harvesting via magnetic induction dampers, which can be applied to active control of buildings subjected to earthquake ground motions. The energy harvested from the building inter-story motions was used to power active devices to control the structural vibration. Scruggs and Iwan (Scruggs 2004, Scruggs and Iwan 2005) also proposed a regenerative force actuation (RFA) network using a permanent magnet machine for structural seismic response control. In the proposed RFA network, some devices extracted mechanical energy from structural vibration, while others re-injected a portion of that energy back into the structure to suppress the structural seismic response. Wang *et al.* (2009) proposed a self-powered semi-active magnetorheological (MR) damper applied to an elevated highway bridge for seismic protection. Jung *et al.* (2010) performed a shaking table test to verify a self-powered MR damper powered by a series-wound electromagnetic device for structural control under earthquakes. Recently, energy harvesting from base-isolated structures subjected to earthquake ground motions was numerically and theoretically studied (Cao and Zuo 2014, Lu *et al.* 2014).

However, electromagnetic energy harvesting from earthquake-induced vibrations is still at its infancy stage. The corresponding issues such as energy prediction and high-efficiency energy harvesting circuits have not been addressed yet. So far, experimental validation of the concept of electromagnetic energy harvesting from low-frequency structural vibrations under earthquakes via shaking table tests has rarely been reported. In this paper, a MPEH is proposed for extracting vibration energy of structures to power WSNs. The performance of the MPEH installed in structures subjected to earthquake ground motions is investigated via both analytical analysis and shaking table test. The predictive model for output power and harvested energy estimations is formulated using a linear equivalent single-degree-of-freedom (SDOF) model considering random base excitations. A series of shaking table tests, in which a scaled single-floor steel frame equipped with a MPEH, were carried out to verify the predictive model and assess the performance of the MPEH during earthquakes. Three circuits, namely, resistor circuit, standard energy harvesting circuit (SEHC), and voltage-mode controlled buck-boost converter, were tested in the experimental study. The output power and energy harvesting efficiency of MPEH connected to the three circuits will be assessed using a scaled El Centro earthquake input with peak ground acceleration (PGA) of 0.1 g. A short discussion is made based on the analytical and experimental results.

2. Electromagnetic energy harvesting system

2.1 Configuration

The process of extracting energy from surrounding environments and converting it into usable energy is known as energy harvesting (Park *et al.* 2008). Vibration energy is ubiquitous in civil structures excited by wind, traffic loads and earthquakes, enabling vibration energy harvesting a reliable and sustainable power source for WSNs. Fig. 1 shows a block diagram of electromagnetic energy harvesting system in civil structures. A harvester installed on a civil structure converts structural vibration energy into electricity and deliver it to energy storage element via a properly-designed interface circuit (also known as power conditioning circuit). The extracted electrical energy can be used to power wireless sensors that monitor the structure. The energy flow from external excitation to energy storage element is shown in Fig. 1. The proposed electromagnetic energy harvesting system consists of a MPEH and an energy harvesting circuit and is described in details in the following sections.

2.2 Macroscale pendulum-type electromagnetic harvester

Compared with wind and traffic load conditions, earthquakes often induce vibrations of greater amplitude, leading to larger energy that can be harvested (Elvin *et al.* 2006). Consequently, harvesting structural vibration energy under earthquakes may offer a valuable power source to seismic response monitoring system, particularly considering the possible power outage during and after earthquakes.

This study propose a MPEH to harvest structural vibration energy when the host structure is subjected to earthquake ground motions as well as other dynamic loads. Fig. 2 shows the configuration of the MPEH, composed of a pendulum, a mass, a gearbox and an electromagnetic generator. The rotational speed of shaft is accelerated by the gearbox to drive the electromagnetic generator, resulting in higher power output and efficiency. The MPEH is essentially a SDOF resonant oscillator, whose natural frequency is tuned close to one of structural natural frequencies by adjusting the pendulum length. As earthquake energy mainly distributes within 0.2 Hz to 10 Hz, seismic responses of structures are most likely dominated by the first several vibration modes of structures. As a result, the MPEH is tuned to match structural fundamental frequency.

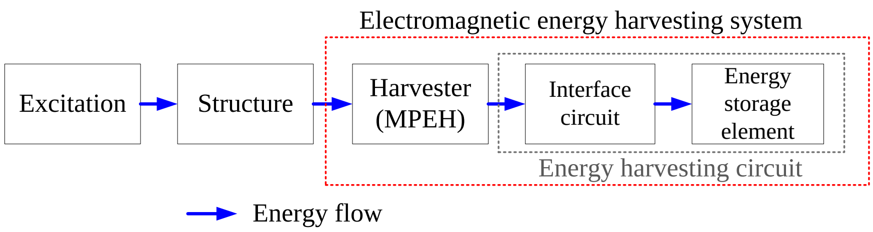

Fig. 1 Block diagram of electromagnetic energy harvesting system in civil structures

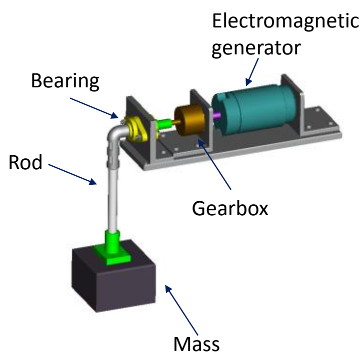

Fig. 2 Macroscale pendulum-type electromagnetic harvester

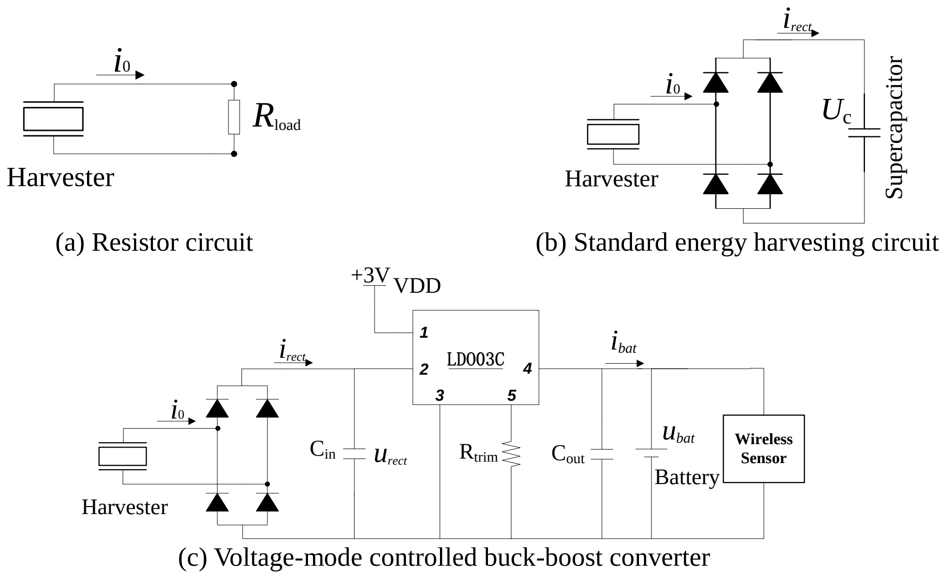

Fig. 3 Energy harvesting circuits

2.3 Energy harvesting circuits

Resistor circuit is employed to represent an ideal energy harvesting circuit, in which energy dissipated in resistor is regarded as the harvested energy, as shown in Fig. 3(a). Although resistor circuit is not a practical energy harvesting circuit, the behaviors of energy harvesters connected with resistor circuits are widely investigated for understanding their fundamental principles and optimal design rules.

Supercapacitors or rechargeable batteries are often used as energy storage elements in practical energy harvesting circuits. Supercapacitors is a new technology to achieve large capacitances typically ranging from 1F to 100F (Casciati and Rossi 2007). Supercapacitors require very simple interface circuits for charging and are able to withstand very high charge and discharge rates. Besides, supercapacitors do not suffer from memory effects like some batteries and have virtually very long live time (Mahlknecht 2004, Casciati and Rossi 2007). In this study, a supercapacitor connected to a full-wave bridge rectifier is used as energy storage element, as shown in Fig. 3(b). This simple circuit is often known as SEHC in piezoelectric energy harvesting (Lefeuvre 2006, Liang and Liao 2009).

Compared with supercapacitors, the voltages of rechargeable batteries are more stable during charging process. In addition, rechargeable batteries require simpler power management circuits and are of much higher energy density (Mahlknecht 2004). However, rechargeable batteries usually have stringent charge requirements to avoid potential overcharge that may damage the batteries. Consequently, power electronic circuits are commonly used to transform AC power from harvesters to stable DC power before charging rechargeable batteries. In this study, a voltage-mode controlled buck-boost converter (LDOC03- 005W05-VJ) shown in Fig. 3(c) is employed as an energy harvesting circuit. The buck-boost converter can convert fluctuant voltage output from the MPEH to relative stable voltage using voltage feedback control. The allowable input voltage of the buck-boost converter ranges from 3 to 13.8 V, and its output voltage can be set from 0.59 V to 5.1 V with maximum output current of 3 A.

3. Predictive model for energy estimation

3.1 Energy estimation in white noise base motion cases

Assuming a MPEH with minimal swing, the dynamics of a MPEH can be represented by a SDOF linear model. A SDOF linear model subjected to base motions is employed to analyze the power and energy of the MPEH, as shown in Fig. 4. The equation of motion is given by

$$m\ddot{x} + c\dot{x} + kx = -m\ddot{x}_b \tag{1}$$

in which

$$k = \frac{mg}{l}, \quad c = 2m\zeta\sqrt{\frac{g}{l}} \tag{2}$$

where m, c, and k denote the mass, equivalent linear damping coefficient, and equivalent stiffness of the MPEH, respectively; x is the horizontal displacement response of the MPEH relative to the base; g is the local acceleration of gravity, ζ is the damping ratio of the MPEH, l is the length of the pendulum; and $\ddot{x}_{\mathrm{b}}$ is the base acceleration of the MPEH.

Eq. (1) can be rewritten as

$$\ddot{x} + 2\zeta\omega_{\mathrm{n}}\dot{x} + \omega_{\mathrm{n}}^2 x = -\ddot{x}_b \tag{3}$$

where

$$\omega_{\mathrm{n}} = \sqrt{\frac{k}{m}}, \qquad \zeta = \frac{c}{2\sqrt{km}} \tag{4}$$

where ω_{n} is the natural frequency of the MPEH.

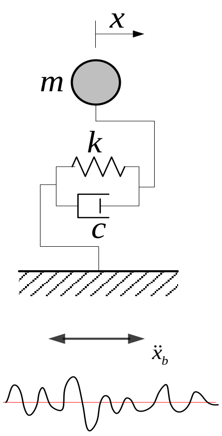

Fig. 4 An equivalent SDOF model for a MPEH

Performing the Fourier transforms of the terms on each side of Eq. (3) offers the velocity complex frequency response function of the SDOF system

$$H_v(j\omega) = \frac{X_v(j\omega)}{X_b(j\omega)} = \frac{-j\omega}{\omega_n^2 - \omega^2 + j2\zeta\omega_n\omega} \tag{5}$$

where $j = \sqrt{-1}$, ω is the frequency of the base acceleration, $X_v(j\omega)$ and $X_b(j\omega)$ are the Fourier transforms of velocity response and the base acceleration, respectively.

The autocorrelation function of base acceleration takes the form

$$R_{\mathrm{b}}(\tau) = E\left[\ddot{x}_{\mathrm{b}}(t)\ddot{x}_{\mathrm{b}}(t+\tau)\right] \tag{6}$$

where τ is the time shift, $E[\cdot]$ denotes the expectation operator. The power spectral density function of the base acceleration $\ddot{x}_{\mathrm{b}}$ is given by

$$S_{\mathrm{b}}(\omega) = \frac{1}{2\pi}\int_{-\infty}^{\infty} R_{\mathrm{b}}(\tau)e^{-j\omega\tau}d\tau \tag{7}$$

Thus, the power spectral density function of velocity response is given by

$$S_{\dot{x}}(\omega) = \left|H_v(\omega)\right|^2 S_{\mathrm{b}}(\omega) \tag{8}$$

The average damping power of the entire SDOF system, i.e., the power absorbed by the MPEH is given by

$$P_{\mathrm{d}} = E\left[p_{\mathrm{d}}(t)\right] = E\left[c\dot{x}^2(t)\right] = c\int_{-\infty}^{+\infty} S_{\dot{x}}(\omega)d\omega = c\int_{-\infty}^{+\infty}\left|H_v(\omega)\right|^2 S_{\mathrm{b}}(\omega)d\omega \tag{9}$$

Random base excitations are generally modeled as white noise processes to simplify the analysis in classical random vibration theory (Yang 1986, Clough and Penzien 1993, Soong and Grigoriu 1993). Consequently, the integral result of Eq. (9) is straightforwardly given by

$$P_{\mathrm{d}} = \pi m S_0 \tag{10}$$

where S_0 represents a constant power spectral density of the base acceleration. The units of S_0 and m in Eq. (10) are $(\mathrm{m/s^2})^2\cdot\mathrm{s/rad}$ and kg, respectively. If the unit of S_0 is taken as $(\mathrm{m/s^2})^2/\mathrm{Hz}$, Eq. (10) should be rewritten in another form

$$P_{\mathrm{d}} = \frac{1}{2}mS_0 \tag{11}$$

Eq. (11) indicates that the power absorbed by the MPEH excited by white-noise base motion is a constant and independent of the damping coefficient c or the damping ratio ζ. The absorbed power is proportional to the power spectral density of base acceleration and the mass of the MPEH. Langley (2014) also investigated the theoretical absorbed power by a SDOF system under random base motion excitations. Eq. (11) is consistent with the formula presented by Langley. A more general conclusion, '*power is proportional to proof mass for any waveform*', was drawn by Mitcheson (2005) when considering base motion input.

Subsequently, Eq. (11) gives an upper bound of output power. Assuming harvesting efficiency known, the average output power of the MPEH is given by

$$P_{\text{out}} = \eta P_{\text{d}} = \frac{1}{2}\eta m S_0 \tag{12}$$

where η is harvesting efficiency. According to Eq. (12), the harvested energy is given by

$$E_h = \int_0^t P_{\text{out}} dt = \frac{1}{2}\eta m S_0 t \tag{13}$$

Eqs. (12) and (13) give output power and output energy prediction if base motions are ideal white noises, respectively. When the base acceleration is a band-limited white noise, Eqs. (12) and (13) are approximate estimations provided that the frequency band is sufficiently wide.

3.2 Energy estimation in earthquake ground motion cases

Structural vibration energy under earthquakes is the energy source considered in this study. The power absorbed by the MPEH under earthquake ground motions can be predicted by Eq. (9) for a given base acceleration power spectral density $S_b(\omega)$.

The MPEH is a resonant-type device, which frequency is tuned to match structural fundamental frequency. Base excitation energy that distributes near MPEH resonance range determines the harvested energy of the MPEH. Therefore, Eqs. (12) and (13) respectively provide handy rough estimations for output power and harvested energy, in which S_0 is the average value of power spectral density $S_b(\omega)$ within a specific narrow band near MPEH resonance range.

4. Efficiency

According to the power flow for an energy harvesting process, the harvesting efficiency takes the form (Zhu *et al.* 2012)

$$\eta = \frac{P_{\text{out}}}{P_{\text{d}}} = \eta_1 \cdot \eta_2 \cdot \eta_3 \tag{14}$$

where η_1 is the electromechanical coupling coefficient that describes the conversion efficiency from mechanical power to electrical power; η_2 stands for the efficiency of electromagnetic generator, which is affected by the power loss induced by coil resistance; and η_3 is the efficiency of energy harvesting circuit.

The three energy conversion ratios are given by

$$\eta_1 = \frac{P_{\text{em}}}{P_{\text{d}}}, \quad \eta_2 = \frac{P_{\text{g}}}{P_{\text{em}}}, \quad \eta_3 = \frac{P_{\text{out}}}{P_{\text{g}}} \tag{15}$$

where P_{p}, P_{em} and P_{g} are the average parasitic damping power, the average electromagnetic damping power and average gross output power from the harvester, respectively. All power terms mentioned in this paper are average power unless otherwise stated.

4.1 Optimal load resistance in resistor circuit cases

In a resistor circuit case, the η_1, η_2 and η_3 of a MPEH are given by

$$\eta_1 = \frac{\zeta_{\mathrm{em}}}{\zeta_{\mathrm{p}} + \zeta_{\mathrm{em}}}, \qquad \eta_2 = \frac{R_{\mathrm{load}}}{R_{\mathrm{coil}} + R_{\mathrm{load}}}, \qquad \eta_3 = 1 \tag{16}$$

where ζ_{p} and ζ_{em} are the parasitic damping ratio and electromagnetic damping ratio, respectively; R_{coil} and R_{load} are coil resistance and load resistance, respectively.

The harvesting efficiency of a MPEH can also be written as (Zhu *et al.* 2012)

$$\eta = \frac{K_{\mathrm{eq}}^2 \alpha}{C_{\mathrm{p}} R_{\mathrm{coil}} (1+\alpha)^2 + K_{\mathrm{eq}}^2 (1+\alpha)} \tag{17}$$

where $\alpha = R_{\mathrm{load}}/R_{\mathrm{coil}}$, $K_{\mathrm{eq}} = K_{\mathrm{em}}\, n_{\mathrm{g}}/l$, K_{eq} denotes the equivalent machine constant of a MPEH, K_{em} denotes the machine constant of electromagnetic rotary generator, n_{g} denotes the amplification ratio of gearbox, C_{p} is equivalent linear parasitic damping coefficient, i.e., $C_{\mathrm{p}} = 2m\omega_{\mathrm{n}}\zeta_{\mathrm{p}}$.

According to Eq. (17), it is straightforward to obtain the optimal load resistance (Zhu *et al.* 2012)

$$R_{\mathrm{opt}} = R_{\mathrm{coil}} \sqrt{1 + \frac{K_{\mathrm{eq}}^2}{C_{\mathrm{p}} R_{\mathrm{coil}}}} \tag{18}$$

4.2 Efficiencies in SEHC cases

If a SEHC used, the η_1, η_2 and η_3 of a MPEH can be expressed as

$$\eta_1 = \frac{\zeta_{\mathrm{em}}}{\zeta_{\mathrm{p}} + \zeta_{\mathrm{em}}}, \qquad \eta_2 = \frac{P_{\mathrm{diode}} + P_{\mathrm{out}}}{P_{\mathrm{coil}} + P_{\mathrm{diode}} + P_{\mathrm{out}}}, \qquad \eta_3 = \frac{P_{\mathrm{out}}}{P_{\mathrm{diode}} + P_{\mathrm{out}}} \tag{19a}$$

in which

$$P_{\mathrm{coil}} = \frac{1}{T_{\mathrm{c}}} \int_{t_0}^{t_0+T_{\mathrm{c}}} i_0^2 R_{\mathrm{coil}}\, dt \tag{19b}$$

$$P_{\mathrm{diode}} = \frac{1}{T_{\mathrm{c}}} \int_{t_0}^{t_0+T_{\mathrm{c}}} 2V_{\mathrm{F}} \cdot i_{\mathrm{rect}}\, dt \tag{19c}$$

$$P_{\mathrm{out}} = \frac{1}{T_{\mathrm{c}}} \int_{t_0}^{t_0+T_{\mathrm{c}}} U_{\mathrm{c}} \cdot i_{\mathrm{rect}}\, dt \tag{19d}$$

where P_{coil} and P_{diode} denote the dissipative power because of copper loss and the bridge rectifier loss, respectively; i_0 is the instantaneous current flowing in the coils of generator; i_{rect} is the instantaneous rectifier output current, $|i_0| \approx i_{\mathrm{rect}}$; V_{F} is the diode forward voltage drop; U_{c} is the voltage of supercapacitor, and T_{c} denotes a calculation period.

4.3 Efficiencies in buck-boost converter cases

In buck-boost converter case, the three energy conversion ratios of a MPEH can be expressed as

$$\eta_1 = \frac{\zeta_{\rm em}}{\zeta_{\rm p} + \zeta_{\rm em}}, \qquad \eta_2 = \frac{P_{\rm diode} + P_{\rm rect}}{P_{\rm coil} + P_{\rm diode} + P_{\rm rect}}, \qquad \eta_3 = \frac{P_{\rm out}}{P_{\rm diode} + P_{\rm rect}} \tag{20a}$$

in which

$$P_{\rm rect} = \frac{1}{T_{\rm c}} \int_{t_0}^{t_0+T_{\rm c}} u_{\rm rect} \cdot i_{\rm rect}\, dt \tag{20b}$$

$$P_{\rm out} = \frac{1}{T_{\rm c}} \int_{t_0}^{t_0+T_{\rm c}} u_{\rm bat} \cdot i_{\rm bat}\, dt \tag{20c}$$

where $P_{\rm coil}$ and $P_{\rm diode}$ can be calculated according to Eqs. (20(b)) and (20(c)), respectively; $P_{\rm rect}$ denotes the output power of rectifier, $u_{\rm rect}$, $u_{\rm bat}$, and $i_{\rm bat}$ denote instantaneous rectifier voltage, instantaneous battery voltage, and instantaneous charging current, respectively.

5. Circuit test

Circuit test is required before shaking table tests. The performance of SEHC has been comprehensively studied by the authors (Zhu *et al.* 2012). Hence, a test of a voltage-mode controlled buck-boost converter (LDOC03-005W05-VJ) was conducted in laboratory.

A prototype circuit was built up on a breadboard and tested in the laboratory, as shown in Fig. 5. The parameters of the voltage-mode controlled buck-boost converter are shown in Fig. 3(c), and the input capacitance $C_{\rm in}$, the output capacitance $C_{\rm out}$ and the Resistance $R_{\rm trim}$ are 15.4 mF, 948.082 nF and 327.5 Ω, respectively. The function of resistor $R_{\rm trim}$ is to set the fixed output voltage of 4.2 V. Based on voltage feedback signal, the output voltage is adjusted to be a stable value by a 1.5 MHz pulse-width-modulator. A DC power is fed into the converter by a DC power supply and the output voltage signal was monitored by an oscilloscope.

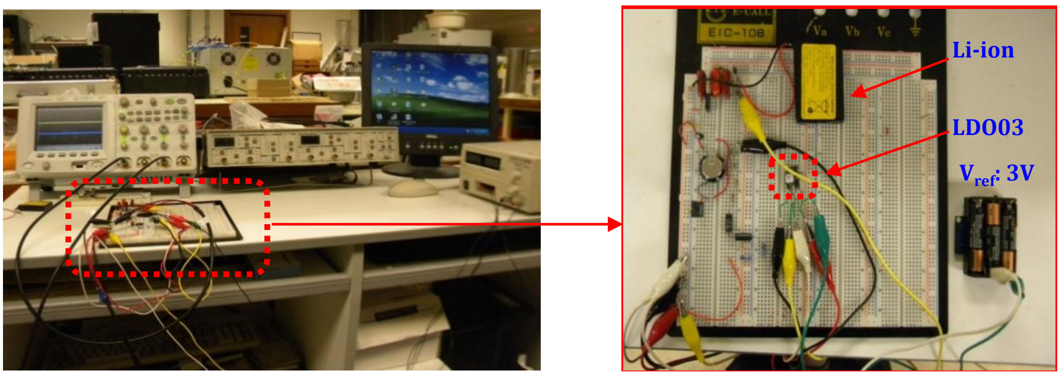

Fig. 5 Lab test setup of buck-boost converter circuit

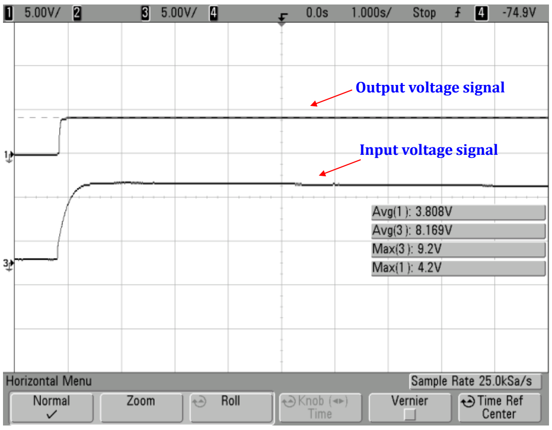

Fig. 6 Input and output voltage of buck-boost converter

Fig. 6 shows that a 9.2 V DC input voltage was successfully converted into the setting value of 4.2V. With this stable voltage output 4.2 V, a Li-ion or NiMH battery can be charged. This will be further investigated in the shaking table tests.

6. Shaking table tests

6.1 Experimental setup

Fig. 7(a) shows the dimensioned drawing of a single-storey steel frame model with a MPEH. Two different test setups were tested in the shaking table tests, as shown in Table 1. The mass and frequency of the single-story steel frame model were set as follows: 527.9 kg and 1.078 Hz in setup 1; 405.3 kg and 1.22 Hz in setup 2. To mimic inherent damping level of steel buildings, an oil damper was fabricated using silicon oil to achieve a practical damping ratios of the steel frame model, i.e., 0.95% and 1.09% in test setup 1 and 2, respectively.

Accordingly, two MPEHs were designed, fabricated, and tested, as shown in Table 1. The frequencies of the two MPEHs are tuned to match the fundamental frequency of steel frame models. A three-phase permanent magnet generator with a length of 94 mm and a diameter of 78 mm was used for power generation.

Table 1 Parameters of single-storey steel frame models and MPEHs

Scenario	Parameters of frame models			Parameters of MPEHs				K_{eq}
	Mass (kg)	Freq. (Hz)	ζ_s (%)	Mass (kg)	Length (mm)	Freq. (Hz)	ζ_p (%)	(V·s/m) (N/A)
Setup 1	527.9	1.078	0.95	17.573	186	1.06	3.8	34.07
Setup 2	405.3	1.236	1.09	5.351	148	1.22	0.6	5.35

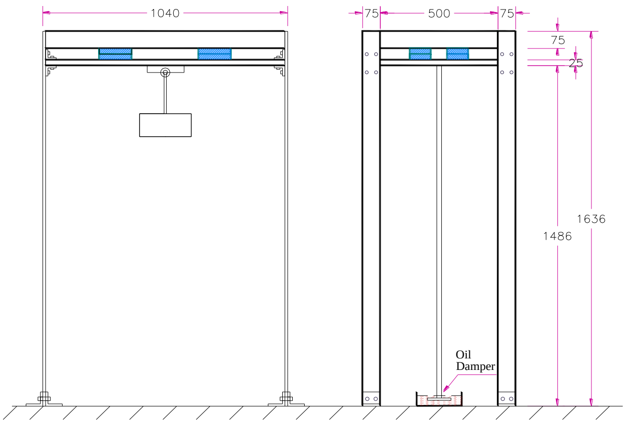

(a) Dimensioned drawing of a single-storey steel frame model with a MPEH

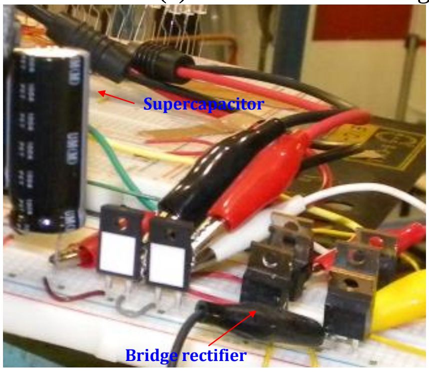

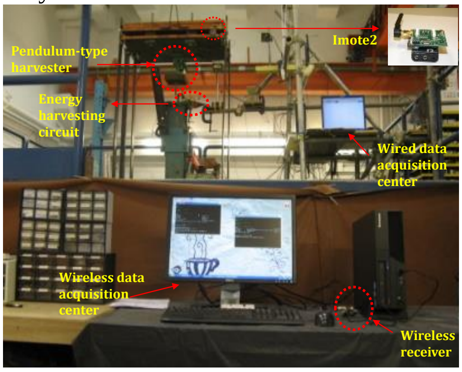

(b) SEHC (c) Test setup on shaking table

Fig. 7 Shaking table experimental setup

The machine constant (K_{em}) of the generator is 0.792 V·s/rad. A gearbox with a ratio of 1:8 was used to accelerate the rational speed of the generator in setup 1. As a result, the equivalent machine constant (K_{eq}) of setup 1 was increased to 34.07 V·s/m, as shown in Table 1. In setup 2, the generator is directly driven by the pendulum without connecting to a gearbox, and consequently its equivalent machine constant (K_{eq}) is less than the counterpart of setup 1, as shown in Table 1.

In the shaking table tests, the MPEHs connect to the four types of circuits as follows:

Open circuit—A three-phase full-wave bridge rectifier was connected to the MPEH under open-circuit condition. The open-circuit voltage was measured when the single-storey steel frame model subjected to the scaled El Centro earthquakes. The output voltage level will be evaluated in this scenario.

Resistor circuit—Three constant resistors, namely, 4 Ω, 34 Ω, and 100 Ω, were connected to the test setup 1, individually. This ideal case was carried out to evaluate the maximum energy harvesting capacity of the MPEH.

SEHC—SEHC circuit was tested by using three different capacitors, namely, 1.5F, 23.5F and 47F, respectively. In order to reduce the rectifier power loss, diodes with ultra-low forward drop voltage V_F (typically 0.25 V) were used to fabricate the full-wave bridge rectifier, as shown in Fig.

7(b). The SEHC circuit was tested in both setup 1 and setup 2.

Buck-boost Converter—The voltage-mode controlled buck-boost converter tested in Section 5 was used in test setup 1. A Li-ion rechargeable battery (nominal voltage of 3.7 V) was connected to the output port of the converter as an energy storage element. The energy harvesting performance was evaluated, and the harvested energy is used to power an Imote2 wireless sensor.

The single-storey steel frame model installed with the MPEHs were tested on a shaking table located at The Hong Kong Polytechnic University. The El-Centro earthquake record scaled to the PGA of 0.1g was employed as the input ground motion in the shaking table tests. The responses of the frame and the MPEH were collected by a KYOWAEDX-100A data acquisition system with a sampling frequency of 100 Hz, including the accelerations of the shaking table and frame, and the currents and voltages within the circuits, as shown in Fig. 7(c).

6.2 Results

The energy harvesting performance of the proposed MPEH with the four types of circuits was evaluated based on the data of the shaking table tests. This section presents the results with respect to output power and energy and energy harvesting efficiency.

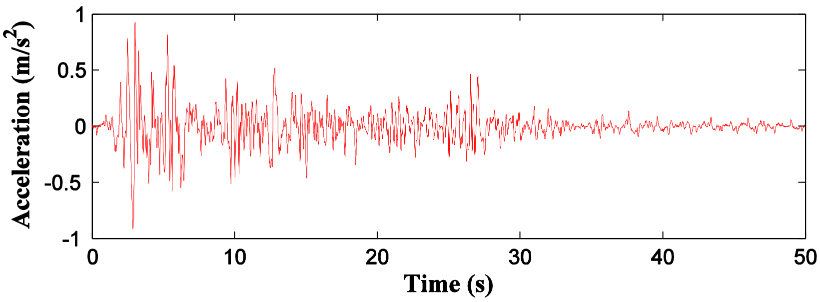

Fig. 8 Ground acceleration time history on the shaking table surface

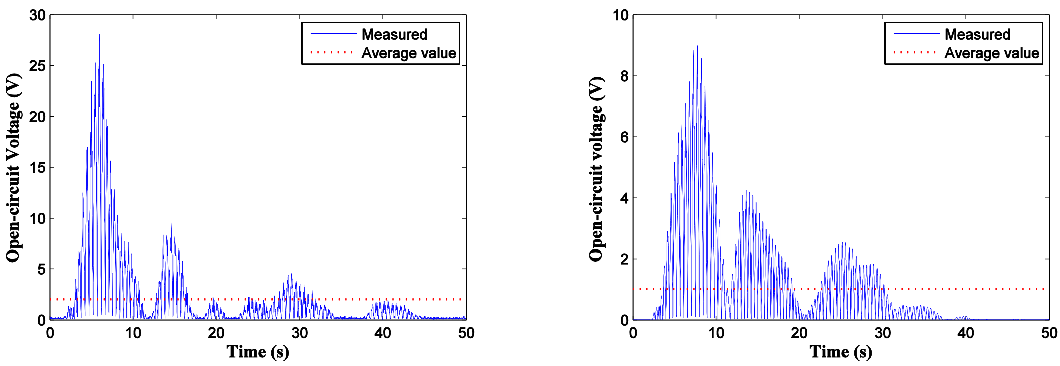

(a) Test setup 1 (b) Test setup 2

Fig. 9 Open-circuit voltages of MPEHs subjected to Scaled El Centro earthquakes

6.2.1 Results of open-circuit case

Fig. 8 shows the ground acceleration time history of the scaled El Centro record measured on the surface of the shaking table. The measured PGA is 0.924 m/s^2, representing a design basis earthquake level in the zone with seismic fortification intensity of 7 degree in China (GB 2010).

Fig. 9 shows the open-circuit voltage time histories, which indicates that the three-phase full-wave bridge rectifier converted the AC voltage to the positive output voltage. The peak and average values of the open-circuit voltage are 28.07 V and 2.03 V, respectively, in test setup 1. Compared with the test setup 1, the open-circuit voltage of test setup 2 is much lower due to smaller mass and smaller equivalent machine constant (K_{eq}), whose peak and average values are 8.99 V and 1.01 V, respectively. The experimental results suggest that the average value of open-circuit voltage is approximately proportional to the square root of harvester mass.

6.2.2 Results of Resistor Circuit Case

Fig. 10(a) shows the acceleration time histories of the steel frame with MPEH setup 1. Since the MPEH setup was hung on the frame, the frame vibration was the input acceleration to the MPEH. The power spectral density of the frame acceleration response was obtained based on the measured data via fast Fourier transform, as shown in Fig. 10(b). A specific frequency band covering the major resonance range of the MPEH (i.e., 0.795 Hz to 1.219 Hz) was selected for calculating the average value of the input acceleration power spectral density. According to Eqs. (12) and (13), the output power and harvested energy were predicted based on the base acceleration power spectral density and theoretical harvesting efficiency. The prediction error shown in Table 2 ranges from 2.4% to 14.04%. Notably, the root mean squares (RMS) of the pendulum rotational angles are 7.6^o, 8.1^o and 9.9^o in the cases of 4 Ω, 34 Ω and 100 Ω, respectively, which suggests that the assumption of minor swing (i.e., rotational angle <10^o) in linear SDOF model were satisfied most of time. However, the peak pendulum rotational angles exceeded the minor swing range in the three cases, e.g., 38.8^o in the case of 34 Ω. This may explain the relatively large error in the prediction based on linear random vibration theory. But in general, the MPEH exhibited a weak nonlinearity in this experiment.

Fig. 11 shows the instantaneous output power of the MPEH connected to a resistor of 34 Ω in test setup 1. The peak output power and average output power are 5969.1 mW and 152.4 mW, respectively. All the results in the resistor circuit cases in test setup 1 are summarized in Table 2. Among the three cases with different resistance, the maximum average output power is 174.5 mW when the load resistance is equal to 100 Ω. Experimental results also reveal that the maximum output power is simultaneously achieved with maximum energy harvesting efficiency, which is consistent with the theoretical analysis. In addition, the total harvested energy is up to 8.72 J when the steel frame model was subjected to the scaled earthquake record with PGA of 0.1 g and duration of 50s. The result represents approximately the maximum achievable electrical energy for the MPEH setup 1 with a mass of 17.573 kg.

Based on the measured output power (P_{out}) and the measured absorbed power (P_d), energy harvesting efficiency can be evaluated according to Eq. (14). A good agreement is observed between the measured energy harvesting efficiency and the theoretical prediction by Eq. (17), as shown in Fig. 12. The theoretical maximum harvesting efficiency of test setup 1 is 37.5% corresponding to the optimal load resistance of 74.8 Ω according to Eq. (18). Similarly, the theoretical curve for test setup 2 can be obtained and is plotted in Fig. 12 as well. The comparison indicates that the theoretical maximum harvesting efficiency of test setup 1 is 50% higher than that of test setup 2. It indicates that a higher equivalent machine constant (K_{eq}) leads to a higher upper bound of harvesting efficiency.

6.2.3 Results of SEHC case

Fig. 13(a) shows a typical charging curve of supercapacitor charged by the electrical energy output from the MPEH in test setup 2. The supercapacitor voltage is charged up from 0.2 V to 0.49 V. Fig. 13(b) shows corresponding charging current curve that varies from 0 A to 0.287 A. The charging current is approximately zero after 31.05 s, resulting in slight drop of the supercapacitor voltage because of leakage. This is because the open-circuit voltage during 31.05 s to 50 s is below 0.579 V, which is less than the sum of the supercapacitor voltage and the forward voltage drop of diode (V_F=0.25 V). Experimental results show that the output power and total output energy are 9.4 mW and 0.47 J in this case, respectively.

Table 3 summarizes the results of SEHC cases in both setup 1 and setup 2. Experimental results indicate that both energy harvesting efficiency and output power are affected by the supercapacitor voltage level. The energy conversion ratios $\boldsymbol{\eta_2}$ and $\boldsymbol{\eta_3}$ depends on the ratio of the supercapacitor voltage to the peak open-circuit voltage (Zhu *et al.* 2012).

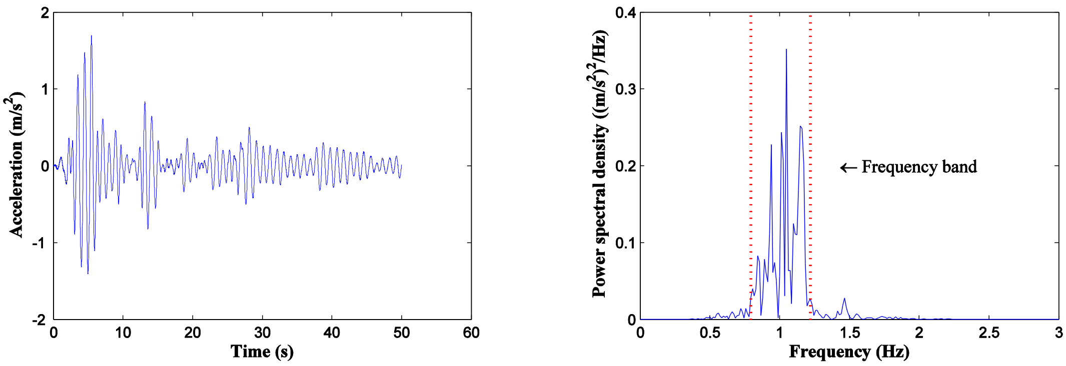

(a) Acceleration (b) Power spectral density

Fig. 10 Accelerations and power spectral density of steel frame model subjected to a scaled El Centro earthquake with the PGA of 0.1 g (Test setup 1)

Table 2 Energy harvesting performance of MPEH with resistor circuits (Test Setup 1)

R_{load} (Ω)	Measured					Predicted		$\frac{\lvert\tilde{P}_{out}-P_{out}\rvert}{P_{out}}$
	E_h (J)	P_{out} (mW)	η (%)	η_1 (%)	η_2 (%)	$\tilde{E}_h$ (J)	$\tilde{P}_{out}$ (mW)	(%)
4	1.64	32.8	7.1	71.9	9.9	1.68	33.6	2.4
34	7.62	152.4	29.7	62.4	47.5	8.69	173.8	14.04
100	8.72	174.5	35.3	50.0	70.5	9.25	184.9	6.0

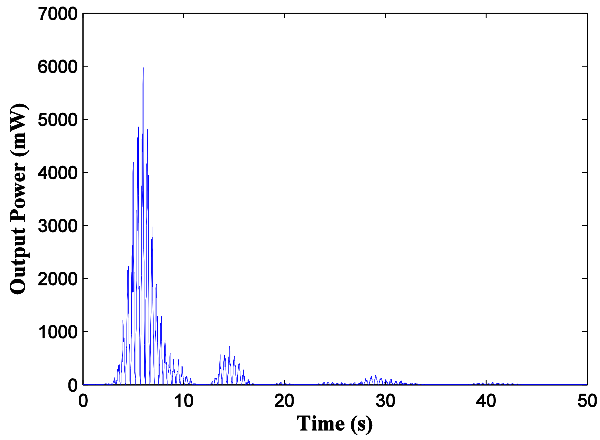

Fig. 11 Instantaneous output power of harvester subjected to Scaled El Centro earthquake with PGA of 0.1 g (Test setup 1)

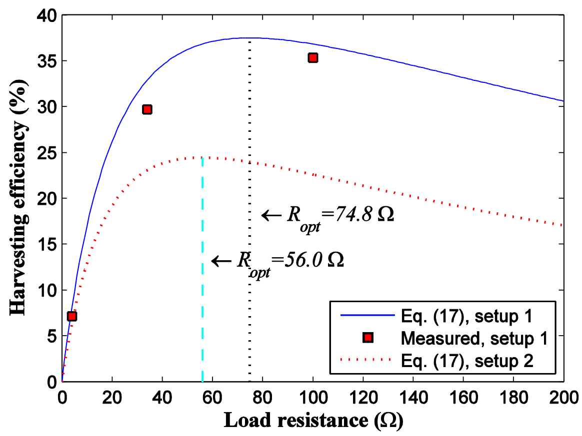

Fig. 12 Comparison between theoretical and measured harvesting efficiency

Table 3 Summary of harvested energy and efficiencies of the MPEHs installed in the single-storey steel frame models subjected to scaled El Centro ground motions (PGA:0.1 g)

Circuit	Test setup	C (F)	U_c (V)	E_h (J)	P_{out} (mW)	η (%)	η_1 (%)	η_2 (%)	η_3 (%)
SEHC	2	1.5	0.20~0.49	0.47	9.4	7.3	83.7	18.1	48.2
SEHC	2	47	0.69~0.78	0.69	13.8	12.4	83.0	23.8	62.6
SEHC	1	23.5	4.01~4.20	2.48	49.6	12.2	24.1	56.3	90.3
Buck-boost	1	/	/	4.67	93.4	16.9	47.2	63.6	56.2

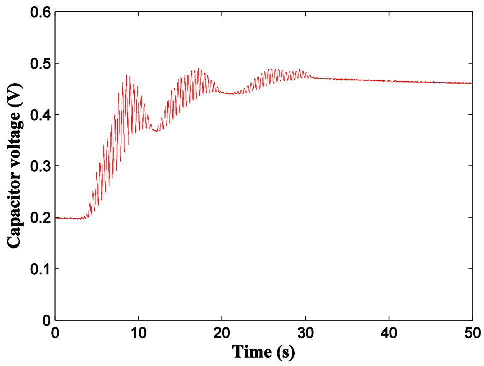

(a) Voltage of supercapacitor

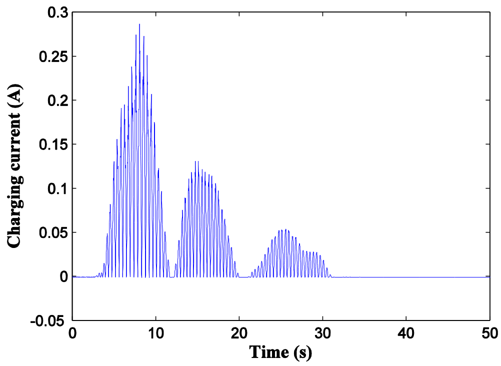

(b) Charging current

Fig. 13 Typical voltage and charging current curves of supercapacitor (Test setup 2, C=1.5F)

When U_c ranges from 0.69 to 0.78 V, the energy conversion ratios η_2 and η_3 increase compared with that of lower supercapacitor voltage, i.e., 0.20-0.49 V. Consequently, the energy harvesting efficiency and corresponding output power is increased up to 12.4% and 13.8 mW, respectively.

The SEHC with a supercapacitor of 23.5 F was tested in test setup 1. The result shows that the output power of 49.6 mW and the harvesting efficiency of 12.2% were achieved, as shown in Table 3. The comparison between the results of setup 1 and setup 2 indicates that the output power rises linearly as the mass increases for a given earthquake ground motion input, which are consistent with the analysis.

6.2.4 Results of buck-boost converter case

A shaking table test of the MPEH connected with the voltage-mode controlled buck-boost converter has been carried out in test setup 1. Fig. 14(a) shows the voltage curve of the Li-ion battery charged through the converter. The battery voltage was charged up from 3.725 V to 3.82 V during the earthquake with PGA of 0.1 g. The battery voltage during energy harvesting process is quite stable, compared with that of SEHC case (Fig. 13(a)).

Fig. 14(b) shows the corresponding charging current curve of the Li-ion battery. The charging current ranges from 0 to 0.268A with a mean value of 0.025A. As a result, the output power is 93.4 mW. The harvested energy by the MPEH is 4.67 J in this case.

The damping ratios of the MPEH with and without the buck-boost converter were identified as 10.1% and 3.8% based on the displacement responses of the MPEH, respectively. Consequently, the electromagnetic coupling coefficient η_1 was calculated as 47.2% according to Eq. (20(a)). The efficiency (η_2) of generator and the efficiency (η_3) of the buck-boost are 63.6% and 56.2%, respectively. As a result, the overall energy harvesting efficiency is 16.9%. Notably, the efficiency of the buck-boost converter in this test is much lower than that of DC power input case, which typically ranges from 91% to 94%. The mismatching of the optimal operation range and the fluctuation of input power may account for the low converter efficiency.

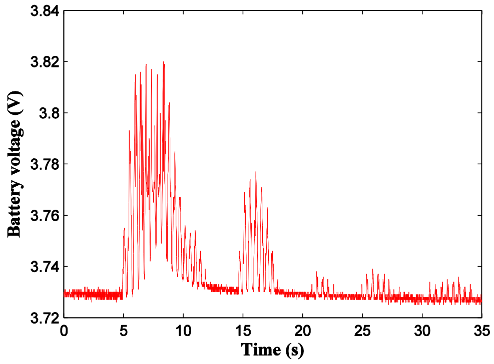

(a) Voltage of battery

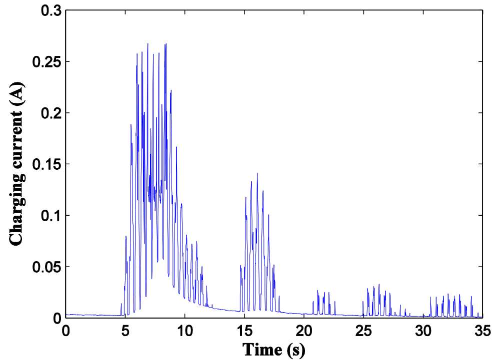

(b) Charging current

Fig. 14 Battery voltage of rechargeable Li-ion battery (Test setup 1)

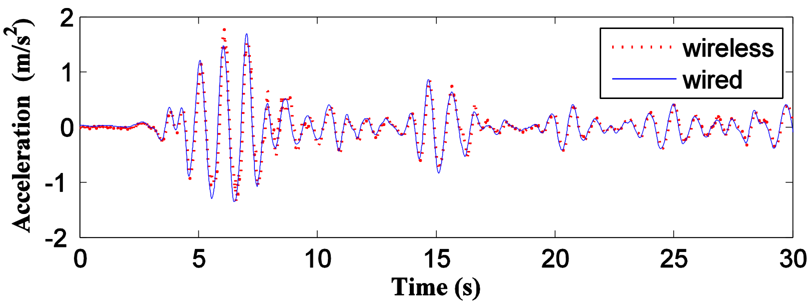

Fig. 15 Comparison of wired and wireless acceleration signals of single-storey steel frame model during El Centro Earthquake (PGA: 0.1 g)

6.2.5 Power wireless sensor

An Imote2 wireless sensor (Rice and Spencer 2008) was used to monitor the dynamic responses of the steel frame model during the scaled El Centro earthquake in test setup 1. In the buck-boost case, the harvested energy was used to charge the Li-ion battery that served as the power supply for the Imote2. The Imote2 consumes approximate 200 mW in the standby state and approximate 620 mW in the sensing state. Therefore, the output power of the MPEH with a mass of 17.573 kg cannot fully power an Imote2 during the scaled El Centro earthquake with PGA of 0.1 g. However, the harvested energy is capable of providing part of electrical energy for wireless sensing.

Fig. 15 shows the comparison between wired and wireless sensing acceleration responses of the single-storey steel frame model subjected to the scaled El Centro earthquake. The Imote2 is capable of sensing structural seismic responses in due course. The wireless sensing signals is of high-quality matching well with the wired sensing signals.

7. Discussion

(1) With respect to Eq. (11), the absorbed power (P_d) of a MPEH is independent of damping coefficient and is a constant for a given base motion input (i.e., structural response). As a result, in order to achieve the maximum output power, the design of a MPEH needs to maximize the energy harvesting efficiency. Based on the analysis of efficiency in ideal resistor circuit case, an impedance-matching strategy that the input resistance of energy harvesting circuit matches the optimal load resistance expressed in Eq. (18) is ready for achieving the maximum energy harvesting efficiency as well as the maximum output power. Energy harvesting circuits with resistive impedance features, such as a fixed duty cycle discontinuous conduction mode buck-boost converter (Lefeuvre *et al.* 2007), can be used to optimize the energy harvesting performance of a MPEH.

(2) Eq. (17) indicates that the lower value of $\boldsymbol{C_{\mathrm{p}} R_{\mathrm{coil}} / K_{\mathrm{eq}}^2}$ leads to a higher energy harvesting efficiency. Using a gearbox is capable to increase the equivalent machine constant K_{eq} with a ratio of $\boldsymbol{n_{\mathrm{g}}^2}$, and increase the parasitic damping (i.e., friction) linearly with the gear ratio n_g, approximately. Consequently, a lower value of $\boldsymbol{C_{\mathrm{p}} R_{\mathrm{coil}} / K_{\mathrm{eq}}^2}$ is achieved by using a gearbox, thus resulting in a higher energy harvesting efficiency. Second, lower parasitic damping (C_p) and lower coil resistance (R_{coil}) also benefit the energy harvesting (Zhu *et al.* 2012). The above two points are also true for a general electromagnetic harvester, whether at microscale or at macroscale.

(3) Extremely uneven energy distribution of base motions within the resonance range of a MPEH may lead to relative large prediction errors when using Eqs. (12) and (13). However, for a given earthquake level, to obtain the mean power spectral density of base accelerations taking into account several earthquake records may compensate the prediction errors to some extent.

(4) The presented predictive model, namely, the output power and harvested energy prediction formulas for a MPEH are also valid for a general linear SDOF harvester.

(5) Supercapacitors have much longer lifetime than rechargeable batteries (Mahlknecht 2004). Consequently, supercapacitors may be more suitable to serve as energy storage elements for vibration energy harvesting during earthquakes considering long return periods of moderate or major earthquakes.

(6) The advantage of the proposed MPEH is that it is capable to provide relatively larger electromechanical coupling coefficient thus enabling higher mechanical-to-electrical energy conversion. With respect to the specially designed configuration, the pendulum motion drives the electromagnetic generator to rotate, and the gearbox accelerates the rotational speed of electromagnetic generator thus amplifying the electrical energy delivered to the external EHC. In this way the proposed MPEH increase both harvested energy and energy harvesting efficiency.

(7) Experimental results indicate that the efficiency of the proposed EHC, including the SEHC and the buck-boost converter, is lower than its optimal value. First, the efficiency of the SEHC varies with the voltage level of supercapacitor according to the theoretical analysis (Zhu *et al.* 2012), which have also been observed in this experiment (see Table 3). Consequently, it is a challenge to maintain the optimal efficiency of the SEHC during the charging process. Second, the efficiency of the buck-boost converter is lower than the theoretical upper limit, which deserves further research in the years ahead.

(8) Although the power harvested by the MPEH cannot fully power the Imote2 in the shaking table test, the amount of harvested energy might be sufficient to power some ultralow-power wireless sensors. For monitoring building behaviors during earthquakes, Torfs *et al.* (2013)

developed a wireless sensor with power consumption of 0.274 mW-1.73 mW, which is less than the output power of the proposed MPEH during a moderate earthquake. Therefore, it is highly potential to implement self-powered wireless sensing using ultralow-power wireless sensors powered by the proposed MPEH during earthquakes, but it needs further experimental validation.

8. Conclusions

This paper proposes an MPEH for harvesting low-frequency vibration energy of civil structures during earthquakes and powering WSNs. A series of shaking table tests has been performed to investigate the energy harvesting performance of the MPEHs installed in a single-story frame subjected to scaled El Centro earthquakes with the PGA of 0.1 g. In ideal resistor circuit cases, experimental results show that a total of 8.72J output energy with the efficiency of 35.3% was harvested by an MPEH with a mass of 17.573 kg during the 50s earthquake period. In more practical cases, under the same conditions, the MPEH harvested 2.48J and 4.67J electric energy via a SEHC and a voltage-mode controlled buck-boost converter, respectively. Therefore, the feasibility of the proposed electromagnetic energy harvesting at low frequency during earthquakes has been demonstrated.

Theoretical models establish optimal design rules and provide predictive capabilities for output power, harvested energy and energy harvesting efficiency. The experimental results indicate that the proposed models are capable of providing rough estimation for output power and harvested energy. Practical applications of electromagnetic energy harvesting from low-frequency structural vibrations during earthquakes demand field demonstration. To improve the energy harvesting efficiency may be one of the major challenges that are facing.

Acknowledgements

The authors are grateful for the financial support from the Research Grants Council of Hong Kong through a GRF grant (Project No. 533011) and from the National Natural Science Foundation of China (Grant Nos.: 51508217 & 51178203), and from the Fundamental Research Funds for the Central Universities (HUST: 2015QN137). The authors would also like to thank the anonymous reviewers for their constructive comments and suggestions.

References

Alavi, A.H., Hasni, H., Lajnef, N., Chatti, K. and Faridazar, F. (2016), "An intelligent structural damage detection approach based on self-powered wireless sensor data", *Automat. Constr.*, **62**, 24-44.

Auge, L.J. (2003), "*Structural magnetic induction dampers in buildings*", Master thesis, Massachusetts Institute of Technology, USA.

Cao, M. and Zuo, L. (2014), "Energy harvesting from building seismic isolation with multi-mode resonant shunt circuits", *Proceedings of the ASME*, San Antonio, TX, USA.

Casciati, F. and Rossi, R. (2007), "A power harvester for wireless sensing applications", *Struct. Control Health*., **14**(4), 649-659.

Clough, R.W. and Penzien, J. (1993), *Dynamics of structures*, 2nd Ed., McGraw-Hill.

Dissertation, California Institute of Technology, Pasadena, California, USA.

Elvin, N.G., Lajnef, N. and Elvin, A.A. (2006), "Feasibility of structural monitoring with vibration powered sensors", *Smart Mater. Struct.*, **15**(4), 977-986.

GB. (2010), "*Code for seismic design of buildings*", GB50011-2010, Beijing, China.

Harb, A. (2011), "Energy harvesting: State-of-the-art", *Renew. Energ.*, **36**(10), 2641-2654.

Jung, H.J., Jang, D.D., Lee, H.J., Lee, I.W. and Cho, S.W. (2010), "Feasibility test of adaptive passive control system using MR fluid damper with electromagnetic induction part", *J. Eng. Mech. - ASCE*, **136**(2), 254-259.

Jung, H.J., Kim, I.H. and Jang, S.J. (2011), "An energy harvesting system using the wind-induced vibration of a stay cable for powering a wireless sensor node", *Smart Mater. Struct.*, **20**(7), 075001.

Jung, H.J., Park, J. and Kim, I.H. (2012), "Investigation of applicability of electromagnetic energy harvesting system to inclined stay cable under wind load", *IEEE T. Magn.*, **48**(11), 3478-3481.

Kim, I.H., Jang, S.J. and Jung, H.J. (2013), "Performance enhancement of a rotational energy harvester utilizing wind-induced vibration of an inclined stay cable", *Smart Mater. Struct.*, **22**(7), 075004.

Lajnef, N., Chakrabartty, S. and Elvin, N. (2008), "A Piezo-powered Floating-gate Sensor Array for Long-term Fatigue Monitoring in Biomechanical Implants", *IEEE Trans. Biomed. Circuits Syst.*,**2**(3)164-172.

Langley, R. (2014), "A general mass law for broadband energy harvesting", *J. Sound Vib.*, **333**(3), 927-936.

Lefeuvre, E., Audigier, D., Richard, C. and Guyomar, D. (2007), "Buck-boost converter for sensorless power optimization of piezoelectric energy harvester", *IEEE T. Power Electr.*, **22**(5), 2018-2025.

Lefeuvre, E., Badel, A., Richard, C., Petit, L. and Guyomar, D. (2006), "A comparison between several vibration-powered piezoelectric generators for standalone systems", *Sensor. Actuat. A: Phys.*, **126**(2), 405-416.

Lei, Y., Tang, Y.L., Wang, J.X., Jiang, Y.Q. and Luo, Y. (2012), "Intelligent monitoring of multistory buildings under unknown earthquake excitation by a wireless sensor network", *Int. J. Distrib. Sens. N.*, **2012**, 914638.

Liang, J.R. and Liao, W.H. (2009), "Piezoelectric energy harvesting and dissipation on structural damping", *J. Intel. Mat. Syst. Str.*, **20**(5), 515-527.

Lu, Q., Loong, C., Chang, C.C. and Dimitrakopoulos, E.G. (2014), "Scavenging vibration energy from seismically-isolated bridges using an electromagnetic harvester", *Proceedings of the SPIE*, 906101-1, San Diego, California, USA.

Lynch, J.P. and Loh, K.J. (2006), "A Summary Review of Wireless Sensors and Sensor Networks for Structural Health Monitoring", *Shock Vib. Digest*, **38**(2), 91-128.

Mahlknecht, S. (2004), "*Energy-self-sufficient wireless sensor networks for the home and building environment*", Ph.D. Dissertation, Universit*ä*t von Pretoria, Wien.

Mitcheson, P.D. (2005), "*Analysis and Optimisation of Energy-Harvesting Micro-Generator Systems*", Ph.D. Dissertation, Imperial College London, London.

Mitcheson, P.D., Green, T.C., Yeatman, E.M. and Holmes, A.S. (2004), "Architectures for vibration-driven micropower generators", *J. Microelectromech. S.*, **13**(3), 429-440.

Park, G., Rosing, T., Todd, M.D., Farrar, C.R. and Hodgkiss, W. (2008), "Energy harvesting for structural health monitoring sensor networks", *J. Infrastruct. Syst.*, **14**(1), 64-79.

Ramadan, K.S., Sameoto, D. and Evoy, S. (2014), "A review of piezoelectric polymers as functional materials for electromechanical transducers", *Smart Mater. Struct.*, **23**(3), 033001.

Rhimi, M. and Lajnef, N. (2012), "Tunable energy harvesting from ambient vibrations in civil structures", *J. Energ. Eng.*, **138**(4), 185-193.

Rice, J.A. and Spencer, B.F. (2008), "Structural health monitoring sensor development for the Imote2 platform", *Proceedings of the SPIE*, San Diego, California, USA.

Roundy, S., Wright, P.K. and Rabaey, J. (2003), "A study of low level vibrations as a power source for wireless sensor nodes" *Comput. Commun.*, **26**(11), 1131-1144.

Sapiński, B. (2011), "Experimental study of a self-powered and sensing MR-damper-based vibration control system", *Smart Mater. Struct.*, **20**(10), 105007.

Sazonov, E., Li, H., Curry, D. and Pillay, P. (2009), "Self-powered sensors for monitoring of highway bridges", *IEEE Sens. J.*, **9**(11), 1422-1429.

Scruggs, J.T. (1999), "*Active, regenerative control of civil structures*", Master Thesis, Virginia Polytechnic Institute and State University, Blacksburg, Virginia, USA.

Scruggs, J.T. (2004), "*Structural control using regenerative force actuation networks*", Ph.D. Dissertation, California Institute of Technology, Pasadena, California, USA.

Scruggs, J.T. and Iwan, W. (2005), "Structural control with regenerative force actuation networks", *Struct. Control Health.*, **12**(1), 25-45.

Shen, W. (2014), "*Electromagnetic damping and energy harvesting devices in civil structures*", Ph.D. Dissertation, The Hong Kong Polytechnic University, Hong Kong.

Shen, W. and Zhu, S. (2015), "Harvesting energy via electromagnetic damper: Application to bridge stay cables", *J. Intel. Mat. Syst. Str.*, **26**(1), 3-19.

Shen, W.A., Lei, Y., Hu, L. and Wang, Y. (2012), "Feasibility of output-only modal identification using wireless sensor network: A quantitative field experimental study", *Int. J. Distrib. Sens. N.*, 2012:560161.

Shen, W.A., Zhu, S. and Xu, Y.L. (2012), "An experimental study on self-powered vibration control and monitoring system using electromagnetic TMD and wireless sensors", *Sensor. Actuat. A: Phys.*, **180**(2012), 166-176.

Soong, T.T. and Grigoriu, M. (1993), "*Random vibration of mechanical and structural systems*", PTR Prentice Hall.

Spencer, B.F., Cho, S. and Sim, S.H. (2011), "Wireless monitoring of civil infrastructure comes of age", *Struct. Mag.*, 12-16.

Torfs, T., Sterken, T., Brebels, S., Santana, J., van den Hoven, R., Spiering, V., Bertsch, N., Trapani D. and Zonta, D. (2013), "Low power wireless sensor network for building monitoring", *IEEE Sens. J.*, **13**(3), 909-915.

Van Noorden, R. (2012), "New year, new science", *Nature*, **481**(7379), 12.

Vullers, R., Schaijk, R., Visser, H., Penders, J. and Hoof, C. (2010), "Energy harvesting for autonomous wireless sensor networks", *IEEE Solid-St. Circ. Mag.*, **2**(2), 29-38.

Wang, Z., Chen Z.Q. and Spencer, B.F. (2009), "Self-powered and sensing control system based on MR damper: presentation and application", *Proceedings of the SPIE Smart Structures/NDE*, 729240.

Williams, C.B. and Yates, R.B. (1996), "Analysis of a micro-electric generator for microsystems", *Sensor. Actuat. A: Phys.*, **52**(1-3), 8-11.

Yang, C.Y. (1986), "*Random Vibration of Structures*", John Wiley & Sons, New York.

Zhu, S., Shen, W.A. and Xu, Y.L. (2012), "Linear electromagnetic devices for vibration damping and energy harvesting: Modeling and testing", *Eng. Struct.*, **34**, 198-212.